JOURNAL NAME
J. Name 2017; **00**:1–??
DOI: X.X/XXXXcnm

CapsidMesh: atomic-detail structured mesh representation of icosahedral viral capsids for the study of their physical properties

J. L. Alonzo-Velázquez[1], S. Botello-Rionda[1], R. Herrera-Guzmán[1], M. Carrillo-Tripp[2†*]

[1]*Ciencias de la Computación, Centro de Investigación en Matemáticas, A.C., Jalisco S/N, Col. Valenciana, C.P. 36023, Guanajuato, Guanajuato, México*
[2]*Laboratorio de la Diversidad Biomolecular, Centro de Investigación y de Estudios Avanzados Unidad Monterrey, Vía del Conocimiento 201, Parque PIIT, C.P. 66600, Apodaca, Nuevo León, México.*

SUMMARY

Viruses are the most abundant pathogens affecting all forms of life. A major component of a virus is a protein shell, known as the viral capsid, that encapsulates the genomic material. The capsid has the fundamental functions to protect and transport the viral genome, and recognize the host cell. Descriptions of this macromolecular complex have been proposed at different scales of approximation, but little is known about the physical properties of the capsid. Here, we introduce a methodology to generate a structured volumetric mesh of icosahedral viral capsids, or CapsidMesh, based on their atomic information. The CapsidMesh models are suitable for numerical simulations and analysis, keeping control over all levels of protein structure (atoms, amino acids, chains, oligomers, capsid). Material properties of the capsid subunits can be set at every mesh element and then run a simulation of a physical process using a third-party package. Analysis can be made by extracting the information of interest. We validated our methodology by generating a CapsidMesh and simulating the nanoindentation through Finite Element analysis of several capsids previously characterized by Atomic Force Microscopy experiments. We estimated the elastic modulus consistently by reproducing the experimental linear elastic response. Our results show that the atomic detail of the CapsidMesh is sufficient to reproduce anisotropic properties of the particle. Supplementary Information available. Copyright © 2017 The Authors

Submitted

KEY WORDS: macromolecular assemblies; virus stability; physical properties

*Correspondence to: E-mail: mauricio.carrillo@cinvestav.mx

Contract/grant sponsor: Consejo Nacional de Ciencia y Tecnología, México.; contract/grant number: 132376 to M.C.-T., and 256126 to R.H.-G.
†Current address: Ciencias de la Computación, Centro de Investigación en Matemticas, A.C., Jalisco S/N, Col. Valenciana, C.P. 36023, Guanajuato, Guanajuato, México

Copyright © 2017 The Authors

1. INTRODUCTION

Viruses are macromolecular complexes made of nucleo-protein components. In the case of icosahedral viruses, at least 60 copies of a specific protein type (VCP) self-assemble into a symmetric closed structure in the form of a hollow shell (capsid) encapsulating the viral genome (DNA or RNA) [1]. Icosahedral capsids display interesting structural features, having a particular topology but a diverse range of VCP folds and particle size. The capsid geometry is commonly described in terms of the so-called symmetry T-number [2]. In recent years, X-ray crystallography and nuclear magnetic resonance (NMR) experiments have produced a considerable amount of structural information with atomic detail [3].

The study of the physical properties that characterize the viral capsid have advanced our knowledge in the fields of structural biology, biotechnology and medicine. In particular, virus nanoindentation produced by Atomic Force Microscopy (AFM) has been used as the standard way to analyze the particle mechanical response [4]. AFM experiments have provided insights into the capsid's molecular structure [5]. From a theoretical standpoint, it has also become possible to study whole viruses by molecular dynamics (MD) methods employing all-atom models [6–9]. In particular, the nanoindentation experiments performed on the *Cowpea Chlorotic Mottle Virus* (CCMV) [10] have been computationally studied to some depth using coarse-grain models [11], elastic network approximations [12], and topology-based self-organized polymer models [13].

Theoretical methods usually provide a higher space resolution than current experimental techniques, yet they tend to have an elevated computational cost. However, the Finite Element Analysis (FEA) theoretical framework is a promising and less expensive alternative approach. An important consideration is that FEA requires a mesh with particular regularity characteristics. Algorithms to generate a biomolecular surface mesh have been previously proposed [14–16]. In general, those meshes are highly optimized for molecular visualization, but are not robust enough for scientific numerical simulation analyses. In the case of viral capsids, some procedures first generate internal and external smooth surface meshes [17], and then generate a non-structured volumetric model by filling the space found between them.

In this work, we present a methodology to build accurate structured volumetric meshes of icosahedral viral capsids based on atomic structural data, taking advantage of the inherent particle symmetries. Our approach has several benefits. 1) It can be systematically used to study the full icosahedral capsid diversity observed in nature [3] under the same framework. Furthermore, since it is geometrically conceived, it can be easily modified to analyze helical capsids as well. 2) Our meshes capture not only the geometry of the capsid but also its topology, i. e., the space between atoms is not artificially filled up, maintaining a porous medium. 3) It is possible to identify and extract the mesh elements associated to any set of atoms, residues or protein subunits, before and after numerical simulations. 4) Specific material parameter values can be set at each mesh element, independent of the structural level of the protein complex, allowing to test any scenario of material interfaces at different structural levels. Finally, to test our methodology, we carried out FEA simulations of the nanoindentation of several viruses previously characterized with AFM allowing us to estimate the elastic modulus of the corresponding capsids with atomic detail. We show that our description is able to reproduce anisotropic properties of the particles.

Copyright © 2017 The Authors

J. Name (2017)
DOI: X.X/XXXXcnm

2. METHODOLOGY

To reduce the computational cost of the mesh generation procedure, we take advantage of the icosahedral symmetry of the virus particle by first meshing a subset of capsid proteins (GMesh). We then rotate images of this subset to generate the mesh of the entire capsid (CapsidMesh). The initial subset of capsid proteins for any icosahedral capsid is the so-called Icosahedral Asymmetric Unit (IAU) [18]. The atomic structural information is specified in a file with the standardized coordinates of the IAU in PDB format [19]. A readily formatted data file can be downloaded from the *Infopage/Biodata* section of the virus of interest at the VIPERdb Science Gateway [3] (Fig. S1). All the DNA or RNA structural information found in the data is discarded. To start, we consider the capsid to be enclosed by the surface of two concentric spheres connected through a radial tesellation projection. Then, we build several concentric intermediate spheres to generate hexahedral volumetric elements, discarding those that do not intersect any atom in the IAU. Images of the surviving hexahedrons are rotated and merged to produce the final structured volumetric mesh of the full capsid. The tessellation resolution can be adjusted to produce high definition meshes. We provide a detailed description of the steps involved in our methodology in the following subsections.

2.1. Fundamental geometric unit (FGU)

Given an icosahedron and a sphere centered at the origin, one can project the edges of the icosahedron radially onto the surface of the sphere, producing an icosahedral tessellation with geodesic triangles (Fig. 1a). Any of the triangular faces of the icosahedron can be used to build the entire icosahedron by applying twenty rotations. The same is true for the icosahedral tessellation of the sphere. Furthermore, we can carry out the same process on a thickened up sphere and obtain an icosahedral tessellation of the shell with radial triangular prisms. We define any of the triangular prisms to be the fundamental geometric unit (FGU). The use of the FGU concept prevents the formation of intersecting mesh elements when the rotations are made later in the process, which is a typical problem found in other methodologies.

2.2. Mesh of the FGU

For simplicity, we first consider a thin FGU. We take one geodesic triangle of the tesellated sphere and give it a structured triangular mesh. We subdivide each equilateral triangle into three non-square quadrilaterals using the barycenter and the midpoint of the three edges. We call this grid the 2D structured-quadrilateral mesh. We project the line segments onto the spherical faces of the FGU. Each quadrilateral of the aforementioned 2D mesh produces two curved quadrilaterals on the curved faces of the FGU, that together make up the top and bottom faces of curved hexahedrons. In order to mesh a thick FGU that contains all the capsid's atoms, we consider it has several layers of equal thickness given by thin FGUs, always using the same structured quadrilateral mesh. The result is the 3D structured hexahedral mesh of the FGU (Fig. 1b). In the example, the FGU's mesh contains $16 \times 3 \times 4 = 192$ hexahedrons, or mesh elements. An increase in mesh resolution will produce smaller hexahedrons and increase the number of mesh elements.

Copyright © 2017 The Authors

J. Name (2017)
DOI: X.X/XXXXcnm

2.3. Geometric icosahedral asymmetric unit (GIAU)

As mentioned before, we use the atomic coordinates of the capsid's IAU as the starting point. To consider all the atom interactions, we construct a capsomere composed of all the adjacent asymmetric units of the IAU (Fig. 2a). In the example shown, we use a T=3 viral capsid. In this case, the IAU contains three identical capsid proteins occupying distinct interaction environments, identified with different labels and colors (according to the standard convention: A in blue, B in red, and C in green). Hence, the final capsomere is composed of 12 equivalent asymmetric units, including the central IAU, with 36 VCPs. We have to do this because we have to account for all the protein-protein contacts inside the IAU, and therefore, the FGU. The thickness of the FGU is defined according to the position of the closest and the farthest atoms from the capsid's geometrical center found in the IAU (plus a threshold value). Therefore, all the atoms found inside the FGU, regardless of what asymmetric unit they belong to, are part of what we call the Geometric Icosahedral Asymmetric Unit, or GIAU (Fig. 2b).

2.4. Radial voxelization of the GIAU

Next, we find all the elements of the structured hexahedral FGU mesh that intersect at least one atom in the GIAU according to criteria explained in the next subsection. We discard those mesh elements that do not comply with this criteria (Fig. 2c). The mesh resolution is a parameter that is set in advance. When its value is high, a mesh with atomic detail is achieved, however, the number of elements increases drastically. In general, it is desirable to find a balance between the volumetric detail and the resolution of the mesh. The final set of mesh elements that are kept will be called GMesh (Fig. 2d).

2.5. Intersection between FGU and GIAU

The volume of an atom of a given type is defined by the characteristic value of its radius. There are several radius definitions [20]. Hence, we consider the atom type radii as parameters whose values can be set in a configuration file. Here, we use the van der Waals radius, defined as half of the internuclear separation of two non-bonded atoms of the same element type on their closest possible approach. We chose this definition since we found that those values give better numerical stability in the simulations compared to other options.

The criteria used to decide whether an hexahedral mesh element intersects a capsid's atom is described in the pseudocode of algorithm 1 and Fig. S2. We perform several tests, where every FGU mesh element e_i is compared to every atom p_j in the GIAU. The variables involved in the tests are the atom radius r_j, the distance d_{ij} between the center of the atom O_j and the barycenter of the mesh element G_i, and the longest distance $\mathbf{a}_i$ between the element's barycenter to a vertex A_i. By doing so, we produce a mesh suitable for numerical simulations and analysis.

2.6. CapsidMesh: mesh of the full capsid

Once the voxelization of the GIAU has been produced and verified for errors, we make images and transform their positions to generate a complete icosahedral particle, according to the set of VIPERdb's standard rotation matrices. The process of merging the GMesh images consists

Copyright © 2017 The Authors

J. Name (2017)
DOI: X.X/XXXXcnm

Algorithm 1 Find mesh elements intersecting the volume defined by the van der Waals atom radius

Require: Array of FGU elements, array of GIAU atoms, and array with van deer Waals radii.

```
for each e_i ∈ {FGU} do
    compute barycenter G_{e_i} of e_i, and distance d_ij
    if d_ij < r^j_vdw then
        element e_i is kept
    end if
    compute max distance a from barycenter G_{e_i} to nodes of element e_i
    for each p_j ∈ {GIAU} do
        compute distance d_ij from G_{e_i} to center of atom p_j
        if d_ij < (r^j_vdw + a) then
            if node of element e_i is inside of atom p_j then
                element e_i is kept
            end if
            if center of atom p_j is inside e_i then
                element e_i is kept
            end if
        end if
    end for
end for
```

of finding all element vertices occupying the same position in space. This is a computationally expensive task. A way to considerably reduce the number of comparisons is to identify which mesh elements are at the interfaces of the FGU and, therefore, the GMesh (Fig. 3a,b). Consequently, in the end we know which hexahedral elements belong to what atom, residue, protein or GMesh interface (Fig. 3c), and the user has complete control over them. At this point, the mesh of the full capsid, or CapsidMesh, is ready to be used in numerical simulations and analysis studies (Fig. 3d). The mesh resolution is a free parameter that the user can configure as needed. This controls the coarseness of the final model (Fig. S3).

2.7. Finite element analysis of CapsidMesh nanoindentation

Here we give a brief description of the theory behind the nanoindentation numerical simulations using the FEA methodology. The relation between strain and stress is deduced from the elasticity property, generally expressed via a constitutive-rigidity matrix

$$D = \frac{E(1-\nu)}{(1+\nu)(1-2\nu)} \begin{bmatrix} 1 & \frac{\nu}{(1-\nu)} & \frac{\nu}{(1-\nu)} & 0 & 0 & 0 \\ \frac{\nu}{(1-\nu)} & 1 & \frac{\nu}{(1-\nu)} & 0 & 0 & 0 \\ \frac{\nu}{(1-\nu)} & \frac{\nu}{(1-\nu)} & 1 & 0 & 0 & 0 \\ 0 & 0 & 0 & \frac{1-2\nu}{(1-\nu)} & 0 & 0 \\ 0 & 0 & 0 & 0 & \frac{1-2\nu}{(1-\nu)} & 0 \\ 0 & 0 & 0 & 0 & 0 & \frac{1-2\nu}{(1-\nu)} \end{bmatrix} \tag{1}$$

given by a symmetric 6×6 matrix which contains the elastic parameters of the medium. In the anisotropic case, it has two independent parameters. For isotopical and homogeneous materials, the two parameters involved in such matrix are the elasticity modulus E and the Poisson coefficient

Copyright © 2017 The Authors

J. Name (2017)
DOI: X.X/XXXXcnm

ν. Note that, for heterogeneous materials, the number of parameters involved may be as large as twenty one. Hooke's law states that

$$\sigma = D\epsilon \tag{2}$$

where σ is the stress and ϵ the strain. The displacement value is modeled by the linear partial differential equation given by Newton's second law:

$$\nabla \cdot \sigma + F = \rho \ddot{\mathbf{u}} \tag{3}$$

where $\mathbf{u}$ is the displacement, F is the force applied per unit of volume, and ρ is the mass density. We can describe the material internal displacements through a discretization of space. Such discretization is achieved by the CapsidMesh. Interpolation of the values of the variables on the nodes of the mesh create a field. Such interpolation is achieved through N_i functions of the form

$$\mathbf{u}(x, y, z) = \sum_i N_i(x, y, z) u_i. \tag{4}$$

Multiplying Newton's second law by some weight functions W_i which are the same as the interpolation functions, known as the Galerkin technique [21], and integrating over the entire domain as well as neglecting the inertia forces, we get the following linear system:

$$K\mathbf{u} = f, \tag{5}$$

generated by the coupling of all the systems given by all the mesh elements, so that K is the standard rigidity matrix of the Finite Element Analysis and f is the vector of forces [21].

This equation must be solved numerically and efficiently with techniques such as LU factorization, iterative methods of preconditioned conjugate gradient, etc. Once the displacements have been obtained, the stresses can be computed at the points of integration by using Eq. 2. Such stresses can be easily extrapolated to the nodes of the mesh using smoothing techniques [21]. One way to understand the effect of the stress tensor with the help of a scalar is to use the von Mises stress J2 [21]

$$J2 = \sqrt{\sigma_x^2 + \sigma_y^2 + \sigma_z^2} - (\sigma_x\sigma_y + \sigma_x\sigma_z + \sigma_y\sigma_z) + 3(\tau_{xy}^2 + \tau_{xz}^2 + \tau_{yz}^2), \tag{6}$$

where $\tau_{xy}, \tau_{xz}, \tau_{yz}$ are the components of the shear stress tensor.

In this way, one can quantify and visualize the effects of the degree of stress in each point of the domain of the mesh. This is an important result since all materials have an equivalent resistance stress with which one can determine how close or how far from failure is each point of the mesh depending on the deformation to which it has been subjected.

3. RESULTS

As mentioned earlier, the mechanical response characterized through AFM nanoindentation experiments performed on the *Cowpea Chlorotic Mottle Virus* (CCMV) [5, 22, 23] have been

Copyright © 2017 The Authors

DOI: X.X/XXXXcnm

computationally studied previously [11, 12, 24]. Given the amount of structural and physical information available, here we take the CCMV capsid as a test case to generate a CapsidMesh with our methodology which can then be used to study the mechanical properties of a macromolecular particle. The same procedure will be used to study other viruses. In particular, the CCMV has an icosahedral capsid, with an outer diameter of 28.8 nm and 4 nm average thickness. Like all T=3 capsids, it is made up of 180 copies of a 190-aminoacids-long protein, organized into 12 pentamers and 20 hexamers.

3.1. Mesh generation

We used our methodology to generate a CapsidMesh of the CCMV capsid based on the atomic Cartesian coordinates of the IAU found in VIPERdb (Fig. S1). The volume is a quantity that can be easily estimated. According to the atomic data, there are 3,574 atoms per IAU $\times$ 60 IAUs = 214,440 heavy atoms in the CCMV capsid (hydrogen data is missing, which is a general fact for structural data obtained by X-ray crystallography). If we consider that the average van der Waals radius of a heavy atom is 1.8Å (0.18nm), each atom has a volume of $(4\pi r^3)/3$ = 24.43Å^3 (0.024nm^3). Therefore, the approximate volume of the CCMV capsid is 5,238,769Å^3 (5,239nm^3). Since the CapsidMesh volume depends on the mesh resolution, we tested a wide range of resolution values; 20.0 - 2.0 Å in 1Å steps, and 2.0 - 0.2 in 0.1Å steps. There is a convergence to the expected volume for resolution values higher than 1Å. Hence, we found that a mesh resolution of 1Å gives accurate atomic detail and is a good compromise with the number of mesh elements and file size.

A previously reported methodology to build low-resolution density maps and triangulated isosurface smoothed meshes, tessellated with tetrahedra, based on the atomic coordinates of a capsid has been used in a series of studies [23–25]. A comparison between the CCMV volumetric mesh generated with such methodology and a mesh generated with the CapsidMesh methodology is shown in Figure 4. The most striking differences are the internal structure regularity and the surface detail of the meshes. The mesh generated with our methodology is structured and reproduces the molecular surface with atomic detail, both on the capsid's interior and exterior, as well as the spaces between protein interfaces. In addition, all the elements in the mesh can be pinpointed and assigned to any structural feature of the particle (Fig. S4). CCMV is a representative case of a T=3 capsid. To test the robustness of our method, we also generated a mesh for a set of representative viral capsids with other T numbers (Fig. S5).

3.2. Nanoindentation numerical simulations

In this work, we combined the CapsidMesh methodology with the FEMT tool [26] to reproduce AFM capsid nanoindentation experiments to test and characterize the mesh generated. The setup of the simulation is depicted in Figure 5. A subset of mesh elements in the south pole are fixed to a solid base plate. Similarly, a subset of mesh elements in the north pole are fixed to a solid cylindrical probe. Both contact points have the same shape as the capsid surface in those points. A force load is then applied downward, and the mesh deformation is measured at every node.

The AFM experiment measures the relation between the applied force and the capsid indentation, i. e., a quantification of the particle's deformation response to squeezing. This produces a characteristic force-indentation profile, or experimental FZ curve, which is later used to estimate the

Copyright © 2017 The Authors

J. Name (2017)
DOI: X.X/XXXXcnm

value of the capsids material properties (Young's modulus, E, or Poisson coefficient ν) by fitting a theoretical model to the collected data using certain approximations. The slope of the FZ curve in the linear regime is defined as the spring constant, k, of the tested material.

It is hard to identify the precise contact point where the piezo touches the capsid in the AFM experiments. If the particle were a perfect sphere, this would not be of importance. However, icosahedral capsids have several symmetry axes (Fig. S6), which in principle, might have different mechanical response properties. Theoretical approaches can address this problem by adjusting the capsid orientation relative to the force load applied. Hence, we performed nanoindentation simulations on three symmetry axes, namely, 2-, 3-, and 5-fold.

In addition to CCMV, we performed nanoindentation simulations of other viruses that had been previously characterized through AFM and whose atomic coordinates were available. It was previously shown that the simulation results are rather insensitive to the value of the Poisson coefficient ν [22]. Using a mesh resolution of 1Å and setting ν to 0.4, we generated a CapsidMesh for the viruses shown in Table I and ran the FEA analysis on them. Since we are working at the linear regime, it is straightforward to find the value of the Young's modulus, E, which reproduces the experimentally measured spring constant k, which in turn results in the corresponding magnitude of the force to be applied to obtain a certain particle indentation. AFM experimental results have shown that forces up to 1nN produce a reversible elastic deformation on the capsid [5]. In this regime, such deformation is not higher than 30% of the particle's radius. Our results are within such range.

4. DISCUSSION

There are several advantages of the CapsdiMesh methodology over previously reported methods to generate mesh models of icosahedral capsids. One is the level of control the user has over each element of the structured mesh. The volumetric meshes produced with our methodology are faithful to the spatial distribution of the atoms and the capsids topological structure, i.e. there are no mesh elements in regions corresponding to empty space between proteins. This is to be contrasted with the meshes produced by [17], for example, where the space between two surface meshes (interior and exterior) are completely filled up. Our meshes have a radial structure built with regular elements and are suitable to be used in numerical analysis methods such as finite element, finite volume and finite differences. Furthermore, one can assign specific material characteristics to each element in the mesh and, therefore, have control over the different structural levels of the macromolecular structure, e. g., atom, residue, oligomer. Our method converts the atomic models to meshes. The simulation and analysis of the meshes are carried out by a third party software. In our case, we used FEMT, however, the way we designed the CapsidMesh methodology offers the flexibility to use other simulation and analysis packages. This independence augments the value of our methodology.

Given that even if a mesh element has a minor intersection with an atom the entire element is accepted into the mesh, the CapsidMesh is always an over-approximation of the actual volume occupancy. This effect is diminished by setting a high resolution value in the current implementation of our methodology. This should not be a problem when regularity in the mesh is a desirable property or does not affect simulations of molecular properties that could be very sensitive to area or volume.

Copyright © 2017 The Authors

J. Name (2017)
DOI: X.X/XXXXcnm

We are working on the implementation of refinement techniques to address problems when that is not the case.

We produced the CapsidMesh of several viruses and performed a simulated nanoindentation on them through FEA. By reproducing experimental AFM measurements, we used our models and methodology to estimate the value of the elasticity modulus, or Young's modulus E, an important macroscopic material property. It is important to note that E might not be the best descriptor to use for a microscopic capsid, since it is not an homogeneous medium and it has an anisotropic character. However, several works have estimated the value of E for CCMV in the past. E estimation seems to highly depend on the approximation used in the continuum model fitted to the experimental data. Both thin-shell and thick-shell models are based on unstructured smooth meshes, and seem to over-estimate the material properties due to a lack of molecular detail in the description of the capsid [22–25]. In any case, the E values predicted with such models are similar to that of rubber or some plastics. The prediction obtained using a CapsidMesh is two orders of magnitude less, consistently for all the cases studied in this work. It is reasonable to say that the difference in this prediction could be a correction in the right direction, since we are dealing with a softer organic substance.

Furthermore, within our approximations, the structural detail of a Capsidmesh is sufficient to obtain anisotropy (Table I). To the best of our knowledge, CapsidMesh is the only model that reproduces the correct relation between symmetry axes in terms of stiffness. AFM experiments showed that the icosahedral axes of T7 capsids follow the relationship $2 > 3 > 5$ [27]. Our prediction for the Bacteriophage T7 Prohead is concomitant with that observation. This result indicates that the use of a mesh with atomic detail is important in the description of macromolecular complexes. With this in mind, and even though we only used CapsidMesh-FEMT to study the nanoindentation process, we expect that the estimation of other biophysical properties will also improve.

5. CONCLUSIONS

In this work, we present a methodology to systematically generate atomic-detailed regular structured volumetric mesh representations of icosahedral capsids based on the structural data readily available in VIPERdb. With the use of a CapsidMesh, it is straightforward to assign a set of mesh elements to any given structural protein level, i. e., from individual atoms to subunits. The CapsidMesh can be coupled to a third party simulation and analysis tool to study physical properties of the particle. In this case, we used FEMT to simulate the nanoindentation process of viral capsids previously characterized through AFM experiments. By reproducing the elastic response through the experimental spring constant, the CapsidMesh-FEMT combination is able to estimate the Young's modulus, showing consistent results with an organic material. In addition, our results show that a mesh with atomic-detail is sufficient to produce an anisotropic model of the icosahedral particles concomitant with experimental results.

ACKNOWLEDGEMENTS

Copyright © 2017 The Authors

DOI: X.X/XXXXcnm

R.H.G. would like to thank the International Centre for Theoretical Physics and the Institut des Hautes Études Scientifiques for hospitality and support. Simulations were executed in the high performance computing center Insurgente from CIMAT.

REFERENCES

1. Cann JA. *Principles of molecular virology*. Elsevier Ac. Press (4th ed.), 2005.
2. Caspar DLD, Klug A. *Physical principles in the construction of regular viruses*. Cold Spring Harbor Laboratory Press, 1962.
3. Carrillo-Tripp M, Shepherd CM, Borelli IA, Venkataraman S, Lander G, Natarajan P, Johnson JE, Brooks CL, Reddy VS. Viperdb2: an enhanced and web api enabled relational database for structural virology. *Nucleic Acid Research* 2009; **37**:D436–D442. URL `http://viperdb.scripps.edu/`.
4. Roos WH, Bruinsma R, Wuite GJL. Physical virology. *Nature Physics* 2010; **6**:733–743.
5. Roos WH, Wuite GJL. Nanoindentation studies reveal material properties of viruses. *Adv. Mater* 2009; **21**:1187–1192.
6. Ayton G, Voth GA. Multiscale computer simulation of the immature hiv-1 virion. *Biophys. J.* 2010; **99**:2757–2765.
7. Miao Y, Johnson JE, Ortoleva PJ. All-atom multiscale simulation of cowpea chlorotic mottle virus capsid swelling. *J. Phys. Chem. B* 2010; **114**:11 181–11 195.
8. Ode H, Nakashima M, Kitamura S, Sugiura W, Sato H. Molecular dynamics simulation in virus research. *Front. Microbiol.* 2012; **3**:1–9.
9. Zhao G, Perilla JR, Yufenyuy EL, Meng X, Chen B, Ning J, Ahn J, Gronenborn AM, Schulten K, Aiken C, *et al.*. Mature hiv-1 capsid structure by cryo-electron microscopy and all-atom molecular dynamics. *Nature* 2013; **497**:643–646.
10. Bancroft JB, Hiebert E. Formation of an infectious nucleoprotein from protein and nucleic acid isolated from a small spherical virus. *Virology* 1967; **32**:354–356.
11. Arkhipov A. Elucidating the mechanism behind irreversible deformation of viral capsids. *Biophys. J.* 2009; **97**:2061–2069.
12. Globisch C, Krishnamani V, Deserno M, Peter C. Optimization of an elastic network augmented coarse grained model to study ccmv capsid deformation. *PLoS ONE* 2013; **8**:e60 582.
13. Kononova O, Snijder J, Brasch M, Cornelissen J, Dima RI, Marx KA, Wuite GJL, Roos WH, Barsegov V. Structural transitions and energy landscape for cowpea chlorotic mottle virus capsid mechanics from nanomanipulation in vitro and in silico. *Biophys. J.* 2013; **105**:1893–1903.
14. Sanner MF, Olson AJ. Reduced surface: an efficient way to compute molecular surfaces. *Biopolymers* 1996; **38**:305–320.
15. Chen M, Lu B. Tmsmesh: a robust method for molecular surface mesh generation using a trace technique. *J. Chem. Theory Comput.* 2011; **7**:203–212.
16. Krone M, Stone J, Ertl T, Schulten K. Fast Visualization of Gaussian Density Surfaces for Molecular Dynamics and Particle System Trajectories. *EuroVis - Short Papers*, Meyer M, Weinkaufs T (eds.), The Eurographics Association, 2012.
17. Si H. Tetgen, a delaunay-based quality tetrahedral mesh generator. *ACM Trans. Math. Softw.* 2015; **41**:1–36.
18. Carrillo-Tripp M, Brooks CL, Reddy VS. A novel method to map and compare protein-protein interactions in spherical viral capsids. *PROTEINS: Structure, Function, and Bioinf.* 2008; **73**:644–655.
19. Berman HM, Westbrook J, Feng Z, Gilliland G, Bhat TN, Weissig H, Shindyalov IN, Bourne PE. The protein data bank. *Nucleic Acids Research* 2000; **28**:235.
20. Housecroft C, Sharpe AG. *Inorganic Chemistry*. Pearson (4th ed.), 2012.
21. Zienkiewicz OC, Morgan K. *Finite elements and approximation*.
22. Michel JP, Ivanovska IL, Gibbons MM, Klug WS, Knobler CM, Wuite GJL, Schmidt CF. Nanoindentation studies of full and empty viral capsids and the effects of capsid protein mutations on elasticity and strength. *PNAS* 2006; **103**:6184–6189.
23. Roos W, Gibbons M, Arkhipov A, Uetrecht C, Watts N, Wingfield P, Steven A, Heck A, Schulten K, Klug W, *et al.*. Squeezing protein shells: How continuum elastic models, molecular dynamics simulations, and experiments coalesce at the nanoscale. *Biophys. J.* 2010; **99**:1175–1181.
24. Gibbons MM, Klug WS. Influence of nonuniform geometry on nanoindentation of viral capsids. *Biophys. J.* 2008; **95**:3640–3649.

Copyright © 2017 The Authors

DOI: X.X/XXXXcnm

25. Gibbons MM, Klug WS. Nonlinear finite-element analysis of nanoindentation of viral capsids. *Phys. Rev. E* 2007; **75**:031 901.
26. Vargas-Felix JM, Botello-Rionda S. Solution of finite element problems using hybrid parallelization with mpi and openmp. *Acta Universitaria* 2012; **22**:14–24. URL `http://www.cimat.mx/~miguelvargas/FEMT/`.
27. Hernando-Perez M, Pascual E, Aznar M, Ionel A, Caston JR, Luque A, Carrascosa JL, Reguera D, de Pablo PJ. The interplay between mechanics and stability of viral cages. *Nanoscale* 2014; **6**:2702–2709.
28. Roos WH, Gertsman I, May ER, III CLB, Johnson JE, Wuite GJL. Mechanics of bacteriophage maturation. *PNAS* 2012; **109**:2342–2347.

6. TABLES

PDBID	T-number	d [Å]	Ind [Å]	Ind/r [%]	F2 [nN]	F3 [nN]	F5 [nN]	k [N/m]	E [MPa]	Ref
- Cowpea Chlorotic Mottle Virus										
1cwp	T3	288	46	0.32	0.55	0.58	0.55	0.119	8.4	[22]
- Human Hepatitis B Virus										
4g93	T4	356	57	0.32	0.37	0.30	0.40	0.070	5.8	[11]
- HK97-like bacteriophage HII										
3j4u	T7	676	108	0.32	0.65	0.47	0.88	0.080	6.4	[28]
- Bacteriophage T7 Prohead										
3izg	T7	548	88	0.32	0.97	0.93	0.88	0.100	12.2	[27]

Table I. Nanoindentation of empty capsids and mechanical properties. Shown: VIPERdb atomic coordinates, particle symmetry, diameter d, nanoindentation produced, deformation percentage, force applied on the 2-fold, 3-fold, and 5-fold axes, spring constant k, Young's modulus E, and experimental FZ curve data used

Copyright © 2017 The Authors

DOI: X.X/XXXXcnm

7. FIGURES

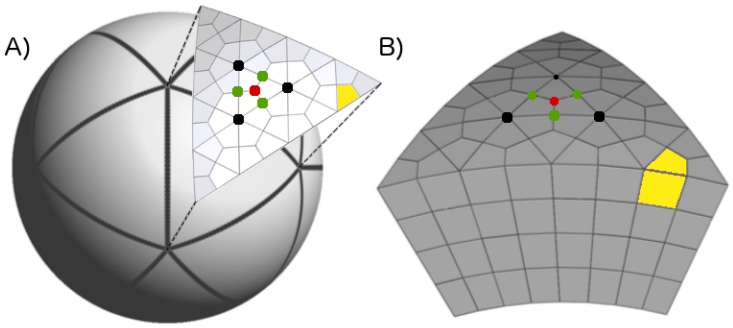

Figure 1. Construction of the fundamental geometric unit (FGU) mesh. (A) Icosahedral tessellation of a sphere with geodesic triangles. One face has been meshed with structured triangles. In this example, the vertices of one of the sixteen triangles on this face are depicted by black dots. Each triangle is subdivided into three non-square quadrilaterals using the baricenter (red dot) and the midpoint of the three edges (gren dots). The result is the 2D structured quadrilateral mesh. (B) Concentric spheres give layers of equal thickness. A radial projection of the face mesh produces structured hexahedrons, or mesh elements (one is highlighted in yellow). This is the 3D structured hexahedral mesh of the FGU.

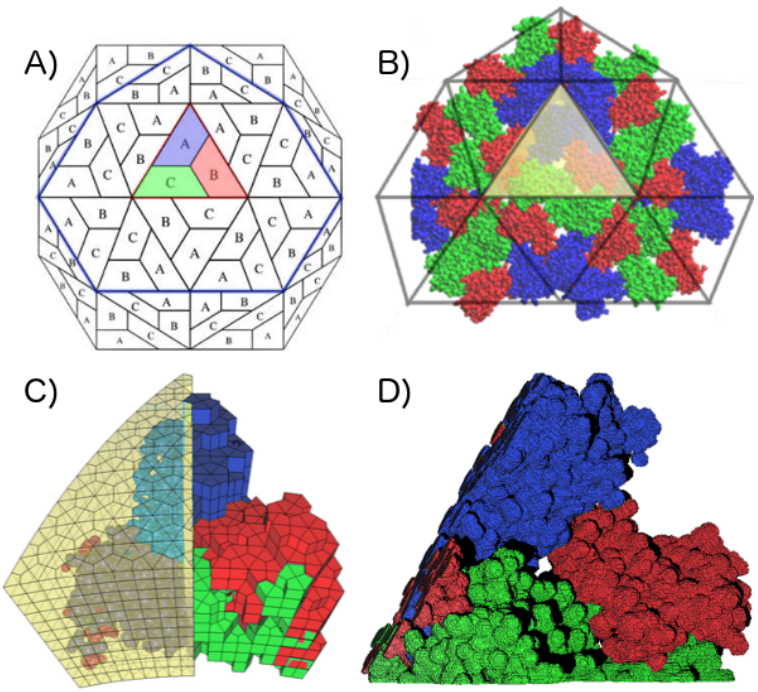

Figure 2. GMesh: construction and voxelization of the Geometric Icosahedral Asymmetric Unit (GIAU). (A) Schematic representation of a full T=3 icosahedral lattice. The central IAU is highlighted in red, and all its adjacent asymmetric units in blue. Each trapezoid represents an independent capsid protein occupying distinct environments, labeled A (blue), B (red), or C (green). (B) Capsomere composed of 12 asymmetric units, 36 capsid proteins. Equivalent environments are depicted by color; A in blue, B in red, and C in green. (C) All the elements in the FGU mesh that intersect an atom in the GIAU are kept, otherwise discarded. An FGU mesh of 5Å resolution is shown. (D) The final set of mesh elements compose the GMesh. A resolution increase to 1Å produces an atom-detailed mesh.

Copyright © 2017 The Authors

J. Name (2017)
DOI: X.X/XXXXcnm

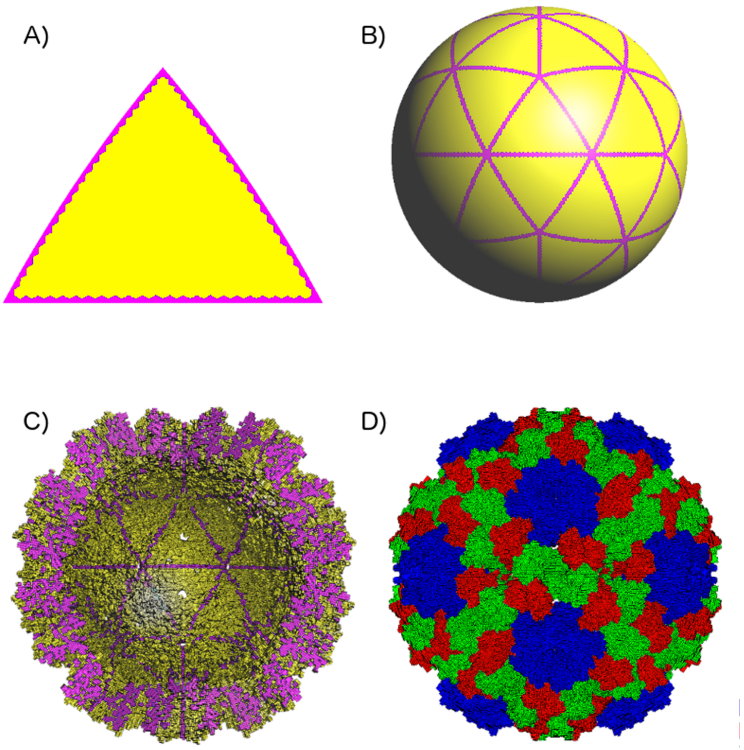

Figure 3. CapsidMesh of a T=3 viral capsid. (A) All the FGU mesh elements at the interfaces are identified, shown in purple. (B) Only those elements are used in the merging of the images process. (C) Inside view of the final volumetric mesh. The GMesh interfaces (purple cells) and the capsid's atomic detail are clear. (D) The CapsidMesh is the final volumetric structured mesh. The hexahedral elements are colored according to the protein environment they belong to (A in blue, B in red, and C in green).

Copyright © 2017 The Authors

DOI: X.X/XXXXcnm

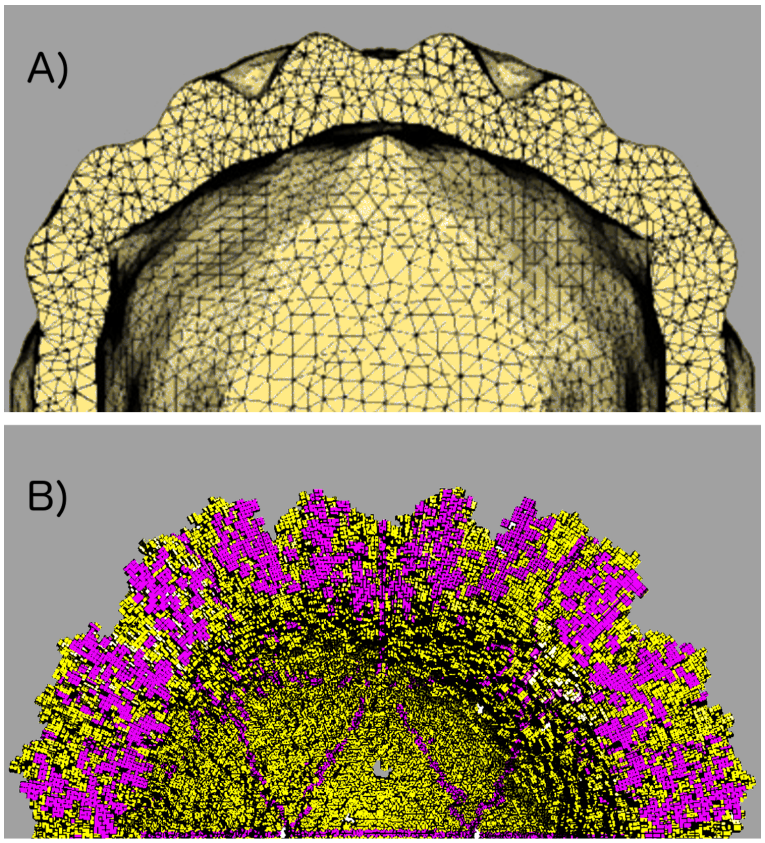

Figure 4. *Cowpea Chlorotic Mottle Virus* capsid. Zoomed in cut view of the 3D mesh created with the (A) method reported by Gibbons and Klug [24], and (B) CapsidMesh method reported in this work. Distinct differences in mesh structure regularity are appreciated. GMesh interfaces in purple.

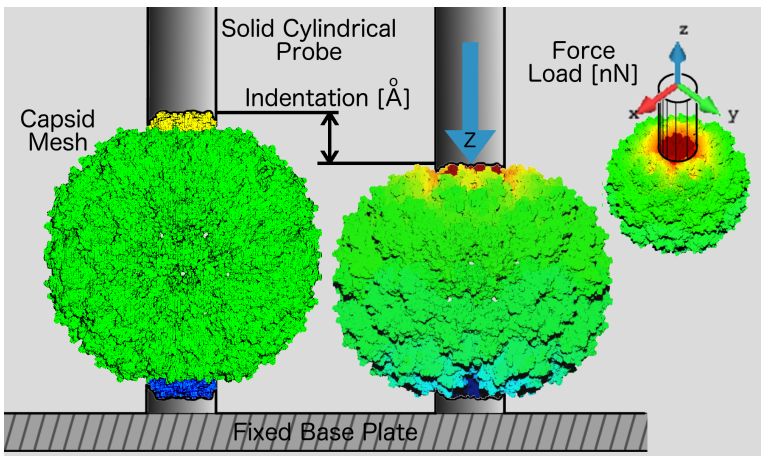

Figure 5. Capsid nanoindentation simulation. Left: Initial conditions, where the mesh elements in blue are fixed to a base plate, and mesh elements in yellow are in contact with a solid cylindrical probe. Right: A force is applied on the contact Z axis over the capsid. The mesh deformation is quantified by the indentation produced and the displacement measured in each element. The color scale used represents minimum displacement in blue, and maximum displacement in red.

Copyright © 2017 The Authors

DOI: X.X/XXXXcnm

8. SUPPLEMENTAL INFORMATION

CapsidMesh: atomic-detail structured mesh representation of icosahedral viral capsids for the study of their physical properties

J. L. Alonzo-Velázquez, S. Botello-Rionda, R. Herrera-Guzmán, and M. Carrillo-Tripp*

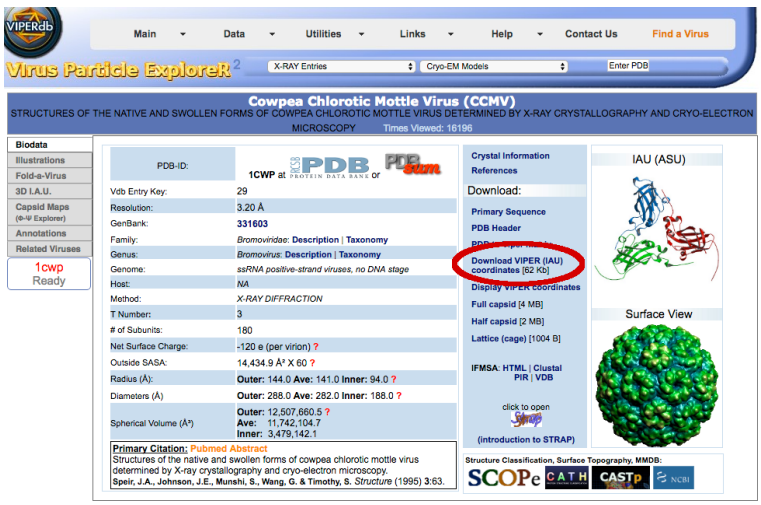

Figure S1. Infopage of a particular virus at the VIPERdb Science Gateway (http://viperdb.scripps.edu/). As an example, we show the data of the *Cowpea Chlorotic Mottle Virus* (PDBID:1CWP). The link to download the standardized atomic coordinates of the IAU is highlighted.

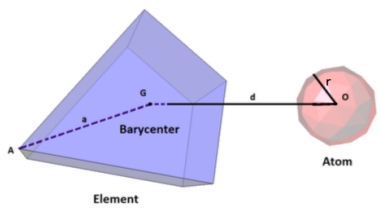

Figure S2. Intersection between FGU elements and GIAU atoms. We perform several tests, where every FGU mesh element e_i is compared to every atom p_j in the GIAU. The values involved in the tests are the atom radius r_j, the distance d_{ij} between the center of the atom O_j and the barycenter of the mesh element G_i, and the longest distance $\mathbf{a}_i$ between the element's barycenter to a vertex A_i.

Copyright © 2017 The Authors

J. Name (2017)
DOI: X.X/XXXXcnm

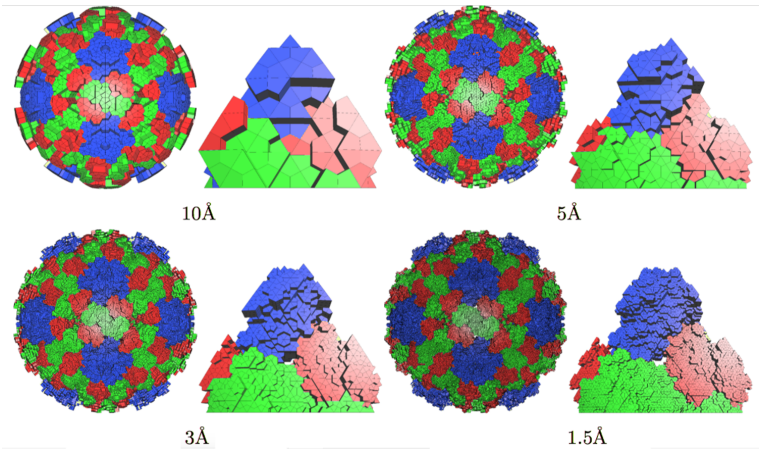

Figure S3. Coarseness of the mesh generated by CapsidMesh. The resolution is a parameter set by the user. Four different resolutions are shown for the same T=3 capsid. The full capsid and the corresponding GMesh are shown for each case. Mesh element color indicates distinct protein environments in the capsid: A in blue, B in red, and C in green.

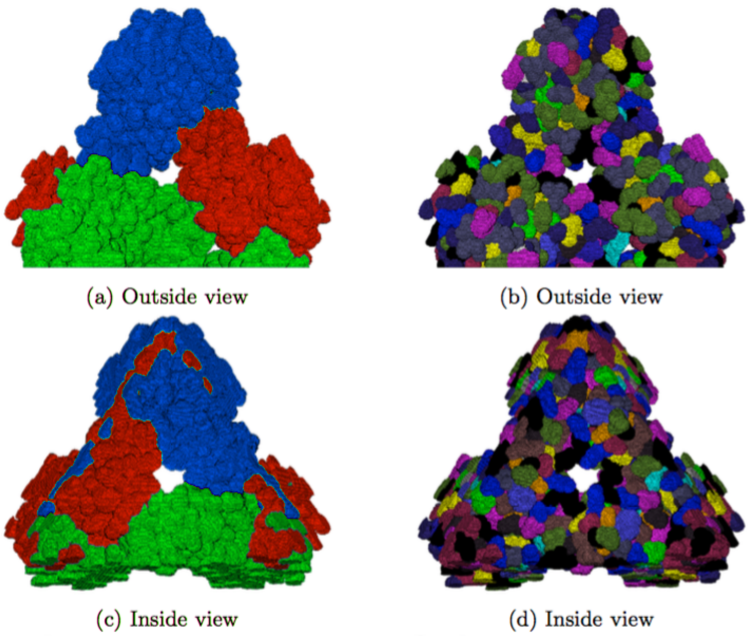

Figure S4. Assignment of specific properties to each element in the mesh. GMesh of the CCMV shown from the outside and from the inside of the capsid. On the left, mesh element color indicates distinct protein environments in the capsid: A in blue, B in red, and C in green. On the right: residues colored by amino acid type.

Copyright © 2017 The Authors

J. Name (2017)
DOI: X.X/XXXXcnm

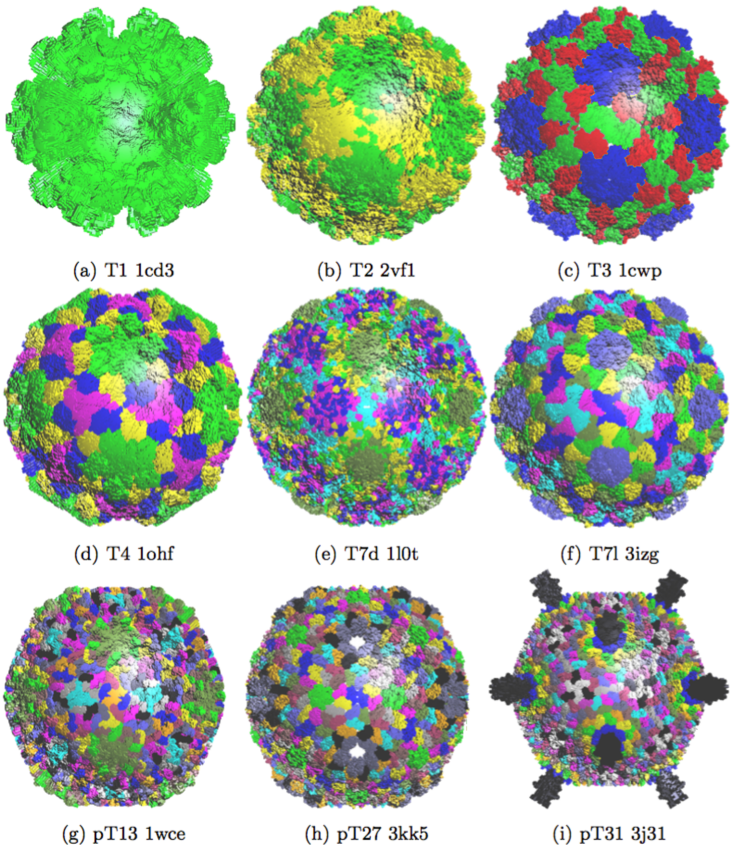

Figure S5. CapsidMesh of a representative set of virus capsids with different T number. The color of each mesh element indicates the location of proteins in different environments inside the capsid. The PDBID and the T-number value is shown under the corresponding mesh.

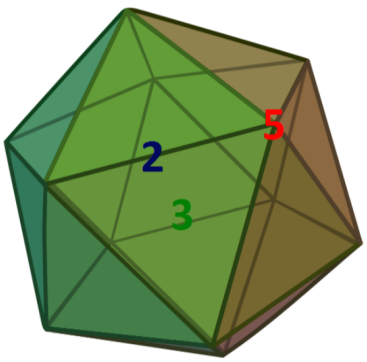

Figure S6. Icosahedral capsids have different symmetry axes. The 2-, 3-, and 5-fold are shown.

Copyright © 2017 The Authors

J. Name (2017)
DOI: X.X/XXXXcnm